Supporting Information

Luchkina et al. 10.1073/pnas.1315769111

SI Materials and Methods

Electrophysiology. Parasagittal hippocampal slices (400 μm) were prepared using standard methods (1). They were placed in a submerged recording chamber after 1- to 4-h recovery and were perfused with extracellular artificial cerebrospinal solution (ACSF) containing (in mM) 124 NaCl, 3 KCl, 1.25 NaH_2PO_4, 1 $MgSO_4$, 26 $NaHCO_3$, 10–15 D-glucose, and 2 $CaCl_2$ and were bubbled with 5% CO_2/95% O_2 at room temperature or at 32 °C. For the recordings of evoked excitatory postsynaptic currents (EPSCs), the CA3 area was removed surgically. Whole-cell voltage-clamp recordings were made from CA1 pyramidal cells, with patch electrodes (3–5 MΩ) containing (in mM) 130 $CsMeSO_4$, 10 Hepes, 0.5 EGTA, 4 Mg-ATP, 0.3 Na-GTP, 5 QX-314, and 8 NaCl; 275–280 mOsm, pH 7.2. Fluorescent neurons were identified under UV illumination with parallel differential interference contrast or bright-field optics. GST and the relevant purified GST-fusion proteins were prepared as described (2) and were included in the intracellular solution at a concentration of 0.5 μM. The PKA inhibitor (PKI) fragment (amino acids 6–22) amide was used in the intracellular solution at a concentration of 0.1 mM.

For the recordings of AMPA receptor-mediated synaptic events, CA1 pyramidal cells were voltage clamped at −70 mV with 100 μM picrotoxin added to the ACSF. For recording of AMPA-mediated miniature EPSCs, 1 μM TTX was included also. Evoked EPSCs were elicited by Schaffer collateral stimulation using a baseline interval of 20 s and intensity adjusted to the minimum strength eliciting a stable response. Recordings were started and afferent stimulation was commenced immediately after obtaining whole-cell access. When indicated, the adenylate cyclase activator forskolin was added to ACSF at a concentration of 50 μM after 5–10 min of baseline recording.

Perforated patch-clamp recordings were made as described previously (3). For these recordings high-resistance electrodes (12–15 MΩ) filled with 130 mM $CsMeSO_4$, 10 mM Hepes, 0.5 mM EGTA, 5 mM QX-314, 8 mM NaCl, and amphotericin B (300 μg/mL) were used, and recordings were started when access resistance was lower than 150 MΩ. Series resistance, input resistance, and holding current were monitored during every sweep (i.e. every 20 s), and cells were discarded if this parameter varied by more than 20%. Under these recording conditions, baseline synaptic transmission remained highly stable (Fig. S2). Long-term potentiation (LTP) was induced 10 min after baseline using a pairing protocol consisting of postsynaptic depolarization (−10 mV) coupled to 10 short bursts (five pulses at 50-Hz given at 5-s intervals) of afferent stimulation. For some of these recordings slices were preincubated for 30 min with the PKA inhibitor KT5720 (2 μM) or the $Ca2^+$/calmodulin-dependent protein kinase II inhibitor KN-62 (3 μM).

Field excitatory postsynaptic potentials (fEPSPs) were recorded in an interface chamber using ACSF-filled electrodes (2–4 MΩ) positioned within the CA1 stratum radiatum. Synaptic responses were evoked every 15 s; the slope of the initial rising phase of fEPSPs (20–80%) was used as a measure of the efficacy of synaptic transmission. Stimulation intensity was adjusted so that the baseline fEPSP slope was 20–40% of the maximal intensity that resulted in the appearance of a population spike. LTP was induced with by tetanic stimulation (100 Hz; 1 s). The PKA inhibitor KT 5720 (1 μM) and/or the CaM kinase II inhibitor KN- 62 (3 μM) were bath applied as indicated. For PKA inhibitor experiments, slices were preincubated in KT 5720 (2 μM) for at least 30 min. The compounds were purchased from Tocris Bioscience, except for amphotericin B (Sigma-Aldrich) and KN-62 and forskolin (Abcam).

Lentivirus Production and Infections. The cDNA encoding rat GluA1 and GluA4 (both as flip isoforms and both with GFP fused to the extracellular N terminus after the signal peptide) (4) were subcloned into the pLen vector containing two separate synapsin1 promoters, the first driving the expression of GFP-tagged AMPA receptor and the second driving separate coexpression of EGFP, using standard methods. The cloned constructs were verified by restriction mapping, and the appropriate size of the encoded recombinant proteins was confirmed by Western blot of transfected HEK293 T cells using rabbit anti-$GluA2/4_{CTDlong}$ (1:2,000) as the primary antibody (4). Lentiviral particles were produced by transfecting HEK293 T cells with Fugene6 (Roche Applied Science) using 0.75 μg of the envelope-coding plasmid pMD.G, 2.25 μg of the packaging plasmid psPAX2, and 3 μg of the relevant pLen transfer vector. Viral particles were harvested 48 h after transfection using PEG-it virus precipitation solution (System Biosciences) and were suspended in PBS.

Lentiviral infections of the CA1 area of 0- to 5-d-old rat pups were made under isoflurane anesthesia essentially as described previously (5). The pups were fixed onto a stereotaxic frame, and 0.02–0.03 mL of lidocaine (20 mg/mL) (Orion Pharma) was injected s.c. The skull was exposed, and small holes were created in each hemisphere using a dental drill. Three injections (each 0.7 μL) of the lentiviral suspension were performed into the hippocampus of each hemisphere. The stereotaxic coordinates for CA1 (with respect to bregma–lambda distance) varied within the following ranges: AP 1.2–1.6, ML 1.2–1.6, DV 1.6–2.0. The wound was treated with Bacibact gel (Orion Pharma) and was sutured, and the pup was left to recover on a heat pad. As soon as the pup was fully recovered, it was returned to its mother. For pain management, the animals were injected s.c. with 0.05 mL of Rimadyl (1 mg/mL) (1:50 dilution in PBS; Pfizer) on the day of operation and on the following 2 d.

Acute slices were cut at P13–P55 and were used for electrophysiological recordings or for analysis of the GluA4 expression level. To estimate the infection rate, slices (250 μM thick) were fixed with 4% (wt/vol) paraformaldehyde for at least 12 h, washed with PBS, stained with 300 nM DAPI in 0.1% Triton X-100 in PBS, and mounted. Images were taken with confocal microscope (Zeiss LSM 5 Pascal with Axioplan 2, using a 25× Plan NEOFLUAR Water immersion objective). The percentage of GFP^+ CA1 pyramidal neurons of DAPI-stained cell nuclei in the CA1 pyramidal layer was determined from a 150 × 150 μm area of a single confocal plane in seven slices from three different animals infected with GFP-GluA4.

Western Blotting. For Western blot assays, the hippocampi were homogenized in ice-cold lysis buffer (150 mm NaCl, 50 mm Tris, 1 mm EDTA, 1% Nonidet P-40, 0.5% deoxycholate, and 0.1% SDS). Protein concentrations were measured using the Bio-Rad DC protein assay (Bio-Rad Laboratories) with BSA as the standard. Samples were boiled at 95 °C in Laemmli buffer (62.5 mm Tris, 1.8% SDS, 7.75% glycerol, and 4.4% 2-mercaptoethanol, pH 6.8) for 5 min. The proteins (15–30 μg per well) were separated by 4–15% SDS/PAGE gels and transferred to Hybond nitrocellulose membrane (GE Healthcare) by a semidry blotting technique. Membranes were blocked for 1 h with 3% (wt/vol) milk in PBS and incubated overnight at 4 °C with primary antibodies:

monoclonal rat anti–α-tubulin (1:5,000, Synaptic Systems), rabbit polyclonal anti-GluA2 (1:1,000, Synaptic Systems), rabbit anti-GluA1$_{CTD}$ (1:2,000) (6). After washing with PBS, membranes were incubated for 1 h at room temperature with HRP-conjugated goat anti-rabbit IgG (1:10 000; GE Healthcare) or anti-rat IgG (1:1,000; Millipore) secondary antibodies. The antibody complexes were visualized using electrochemiluminescence kits (Amersham Biosciences) followed by exposure to a Fuji LAS-3000 camera (Tamro Medlabs) for ECL detection. The integrated optical density (IOD) of protein bands was measured using ImageJ software. To control for differences among samples in total protein concentration, the filters were reblotted with anti–α-tubulin antibodies, and the IOD values were normalized against the level of α-tubulin in the same sample. These corrected IOD values were used for calculation of statistical differences (Student's paired, two-tailed *t* test). For the histograms, the corrected IOD values were normalized further to corresponding controls and averaged (± SEM), with 100% representing no change.

1. Lauri SE, et al. (2006) Functional maturation of CA1 synapses involves activity-dependent loss of tonic kainate receptor-mediated inhibition of glutamate release. *Neuron* 50(3):415–429.
2. Coleman SK, Cai C, Kalkkinen N, Korpi ER, Keinänen K (2010) Analysis of the potential role of GluA4 carboxyl-terminus in PDZ interactions. *PLoS ONE* 5(1):e8715.
3. Luchkina NV, Sallert M, Clarke VRJ, Taira T, Lauri SE (2013) Mechanisms underlying induction of LTP-associated changes in short-term dynamics of transmission at immature synapses. *Neuropharmacology* 67:494–502.
4. Coleman SK, et al. (2006) Isoform-specific early trafficking of AMPA receptor flip and flop variants. *J Neurosci* 26(43):11220–11229.
5. Vesikansa A, et al. (2012) Expression of GluK1c underlies the developmental switch in presynaptic kainate receptor function. *Sci Rep* 2:310.
6. Cai C, Li H, Rivera C, Keinänen K (2006) Interaction between SAP97 and PSD-95, two Maguk proteins involved in synaptic trafficking of AMPA receptors. *J Biol Chem* 281(7): 4267–4273.

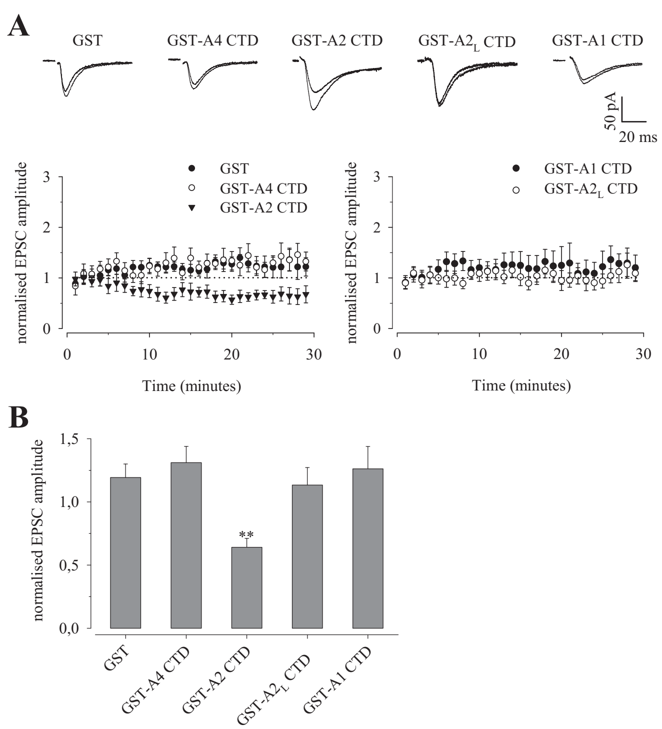

Fig. S1. Long C-terminal domains of AMPA-receptor subunits have no effects on baseline transmission at immature CA3–CA1 synapses. (*A*) Examples of traces (*Upper*) and a time-course plot (*Lower*) illustrate the lack of effect of the postsynaptic application of GST ($n = 9$), GST-GluA4 C-terminal domain (CTD) ($n = 5$), GST-GluA1 CTD ($n = 7$), and GST-GluA2$_L$ CTD ($n = 5$) on EPSCs at immature [postnatal day 4 (P4)–P6] CA3–CA1 synapses. GST-GluA2 CTD was used as a positive control and caused down-regulation of transmission, likely by inhibiting the N-ethylmaleimide-sensitive factor interaction as shown previously in slices from older animals ($n = 5$) (1–3). (*B*) Statistics summarizing the effects of the various fusion proteins on the amplitude of excitatory postsynaptic currents (EPSCs). $^{**}P < 0.001$.

1. Nishimune A, et al. (1998) NSF binding to GluR2 regulates synaptic transmission. *Neuron* 21(1):87–97.
2. Song I, et al. (1998) Interaction of the N-ethylmaleimide-sensitive factor with AMPA receptors. *Neuron* 21(2):393–400.
3. Lüscher C, et al. (1999) Role of AMPA receptor cycling in synaptic transmission and plasticity. *Neuron* 24(3):649–658.

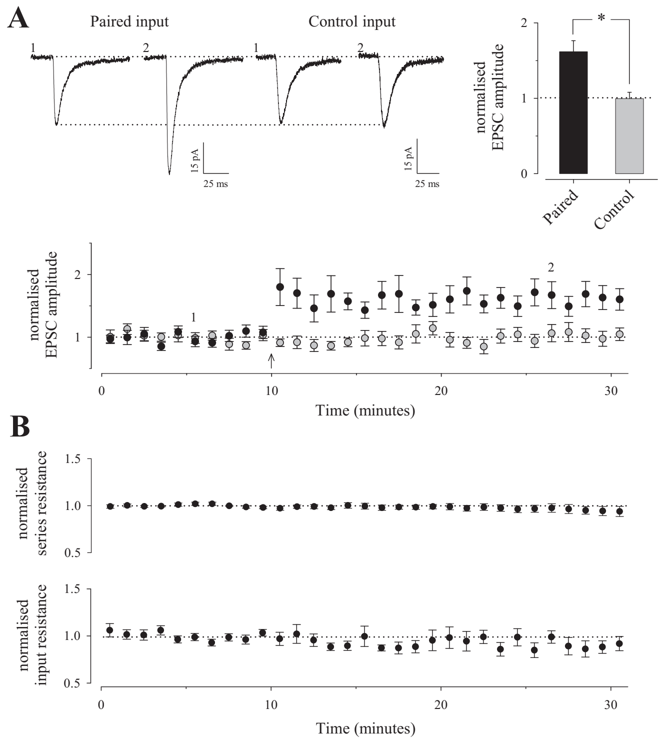

Fig. S2. Perforated patch-clamp recordings from CA1 pyramidal neurons with stimulation of two independent pathways in P5–P8 WT mice (n = 12). (*A*) Examples of traces (*Upper*) and time-course plots (*Lower*) show that the pairing protocol produced a stable pathway-specific LTP. In the control pathways, which were not stimulated during the depolarization of the postsynaptic neuron, no changes in the EPSC amplitude were observed. (*B*) The membrane properties of the recorded neurons were highly stable throughout the experiment.